The EMBO Journal vol.13 no.8 pp.1969 – 1980, 1994

Evidence that the pathway of transferrin receptor mRNA degradation involves an endonucleolytic cleavage within the 3′ UTR and does not involve poly(A) tail shortening

Roberta Binder, Jill A.Horowitz[1], James P.Basilion, David M.Koeller[2], Richard D.Klausner and Joe B.Harford[3,4]

Cell Biology and Metabolism Branch, NICHD, NIH, Bethesda, MD 20892, USA
[1]Present address: Division of Hematologic Products, CBER, FDA, Bethesda, MD 20892
[2]Present address: Department of Pediatrics, University of Colorado Health Sciences Center, Denver, CO 80262
[3]Present address: RiboGene Inc., 21375 Cabot Boulevard, Hayward, CA 94545, USA

[4]Corresponding author

Communicated by I.W.Mattaj

The stability of transferrin receptor (TfR) mRNA is regulated by iron availability. When a human plasmacytoma cell line (ARH-77) is treated with an iron source (hemin), the TfR mRNA is destabilized and a shorter TfR RNA appears. A similar phenomenon is also observed in mouse fibroblasts expressing a previously characterized iron-regulated human TfR mRNA (TRS-1). In contrast, mouse cells expressing a constitutively unstable human TfR mRNA (TRS-4) display the shorter RNA irrespective of iron treatment. These shorter RNAs found in both the hemin-treated ARH-77 cells and in the mouse fibroblasts are shown to be the result of a truncation within the 3′ untranslated regions of the mRNAs. The truncated RNA is generated by an endonuclease, as most clearly evidenced by the detection of the matching 3′ endonuclease product. The cleavage site of the human TfR mRNA in the mouse fibroblasts has been mapped to single nucleotide resolution to a single-stranded region near one of the iron-responsive elements contained in the 3′ UTR. Site-directed mutagenesis demonstrates that the sequence surrounding the mapped endonuclease cleavage site is required for both iron-regulated mRNA turnover and generation of the truncated degradation intermediate. The TfR mRNA does not undergo poly(A) tail shortening prior to rapid degradation since the length of the poly(A) tail does not decrease during iron-induced destabilization. Moreover, the 3′ endonuclease cleavage product is apparently polyadenylated to the same extent as the full-length mRNA.

Key words: endonuclease/mRNA stability/poly(A) tail/ribonuclease/transferrin receptor mRNA

Introduction

The importance of mRNA stability as a control point in eukaryotic gene regulation is now abundantly clear (for review see Belasco and Brawerman, 1993; Sachs, 1993). The half-lives of many mRNAs are modulated in response to exogenous stimuli, position in the cell cycle or state of differentiation. In fact, cellular mRNA levels often correlate more closely with transcript stability than with transcription rate. However, compared with transcription, considerably less is known concerning the factors and processes by which control of mRNA stability is achieved.

Dividing cells of higher eukaryotes acquire iron via a high affinity receptor for the plasma iron-carrying protein, transferrin. The level of expression of the transferrin receptor (TfR) is the determinant of the rate of iron acquisition and TfR expression is highly regulated by iron (Harford, 1993; Klausner *et al.*, 1993). The regulation of TfR expression is accomplished primarily post-transcriptionally through modulation of the stability of the TfR mRNA (Harford, 1993), which displays a relatively short half-life (~45 min) when iron is abundant and a relatively long half-life (>>3 h) when iron is scarce (Koeller *et al.*, 1991). The modulation of TfR mRNA stability is mediated by its 3′ untranslated region (UTR), which contains a rapid turnover determinant (Müllner and Kühn, 1988; Casey *et al.*, 1989) and RNA motifs termed iron-responsive elements (IREs) that are recognized by a cytoplasmic IRE binding protein (IRE-BP). The interaction of the IRE-BP with a single IRE within the 5′ UTR of ferritin inhibits translation of the ferritin mRNA (Casey *et al.*, 1988b; Leibold and Guo, 1992; Klausner *et al.*, 1993). In the case of the TfR mRNA, which contains five IREs within its 3′ UTR, an analogous interaction inhibits degradation of the transcript, presumably by functionally masking the rapid turnover determinant (Casey *et al.*, 1989).

Although the IRE–IRE-BP interaction is one of the better characterized components of a system for post-transcriptional gene regulation, many of the details of the mechanisms involved in the regulation of TfR mRNA turnover remain obscure. As with most systems involving mRNA degradation, very little is known about the nuclease(s) involved or the actual pathway of degradation. In general, mRNA degradation occurs with few, if any, intermediates in the breakdown process detected. This observation is thought to reflect a relatively slow rate-determining step to initiate mRNA degradation followed by very rapid destruction of the product(s) of this initial step. Here we document the appearance of a truncated TfR RNA species during the iron-regulated degradation of the human TfR mRNA in a human plasmacytoma cell line and in mouse fibroblasts expressing an iron-regulated human TfR mRNA. Moreover, in mouse fibroblasts expressing a constitutively unstable form of the human TfR mRNA, the truncated form of the TfR RNA is constitutively present. Evidence is presented indicating that the truncated RNA is the product of an endonucleolytic cleavage at a specific site within the previously defined regulatory region of the TfR mRNA. We also show that the endonucleolytic cleavage occurs without detectable alteration in length of the poly(A) tail of the TfR mRNA.

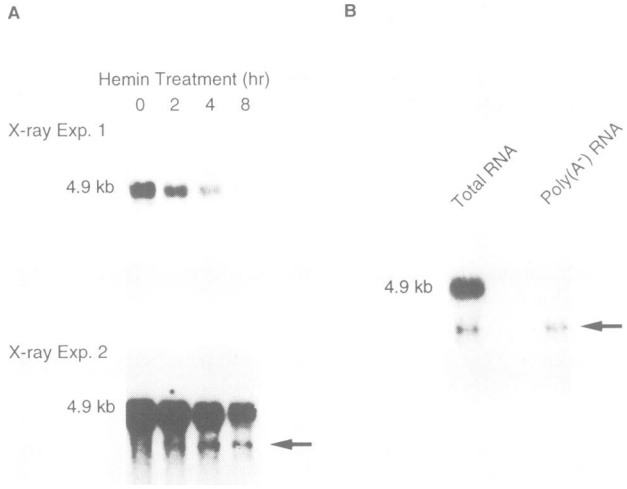

Fig. 1. TfR mRNA from ARH-77 cells exhibits a hemin-dependent shorter RNA that lacks a poly(A) tail. (**A**) RNA samples (10 μg) from ARH-77 cells treated with hemin (100 μM) for the times indicated, were electrophoresed through a 1.2% agarose−2.2 M formaldehyde gel and blotted to a nylon filter. The nylon filter was hybridized with 1×10^6 c.p.m./ml of a 2.6 kb *Eco*RV to *Bam*HI fragment of plasmid TRS-1 (Probe I, Figure 2A) that had been random-primed in the presence of [α-^{32}P]dCTP. Shown are a short (X-ray Exp. 1) and long (X-ray Exp. 2) autoradiographic exposure of the same nylon filter. Full-length 4.9 kb TfR mRNA and truncated TfR RNA (arrow) are indicated. Based on comparison with the migration of the 4.9 kb TfR mRNA and the 28S and 18S ribosomal RNAs, the shorter TfR RNA is estimated to be ~3.6 kb in length. (**B**) RNA from the 6 h hemin time point was subjected to oligo(dT) cellulose chromatography. Total mRNA (10 μg) and the corresponding poly(A)$^-$ fraction (flow through) were subjected to electrophoresis, blotting and hybridization as described in panel A.

Results

We (Koeller *et al.*, 1991) and others (Müllner and Kühn, 1988) have shown that the regulation of human TfR mRNA levels by iron is the consequence of an alteration in the stability of the mRNA, with its half-life varying from ~45 min in mouse fibroblasts replete with iron to much greater than 3 h in cells treated with an iron chelator (Koeller *et al.*, 1991). We have observed that various cell lines differ in terms of whether iron chelator or iron source results in the most marked effect on TfR mRNA stability (when compared with no treatment). In ARH-77 cells, a human plasmacytoma cell line, treatment with the iron chelator desferrioxamine causes little or no change in TfR mRNA level (data not shown), but treatment of these cells with hemin (ferric protoporphyrin IX) results in a marked decrease in the level of mRNA encoding the TfR (Figure 1A, upper panel). A longer autoradiographic exposure of the same Northern blot (Figure 1A, lower panel) reveals that, as the full-length TfR mRNA is degraded, a shorter TfR RNA appears. The kinetics of the appearance of the shorter RNA suggested that it might be a meta-stable product of the degradation process.

Detectable intermediates in mRNA turnover have been reported in but a few instances. The characterization of such intermediates can be revealing as to the pathway of mRNA decay and may provide information regarding the specificity of the RNases involved. The shorter, hemin-dependent TfR RNA in ARH-77 cells was estimated by comparison with the migration of ribosomal RNAs to be approximately 1−1.5 kb shorter than the full-length 4.9 kb TfR mRNA. The

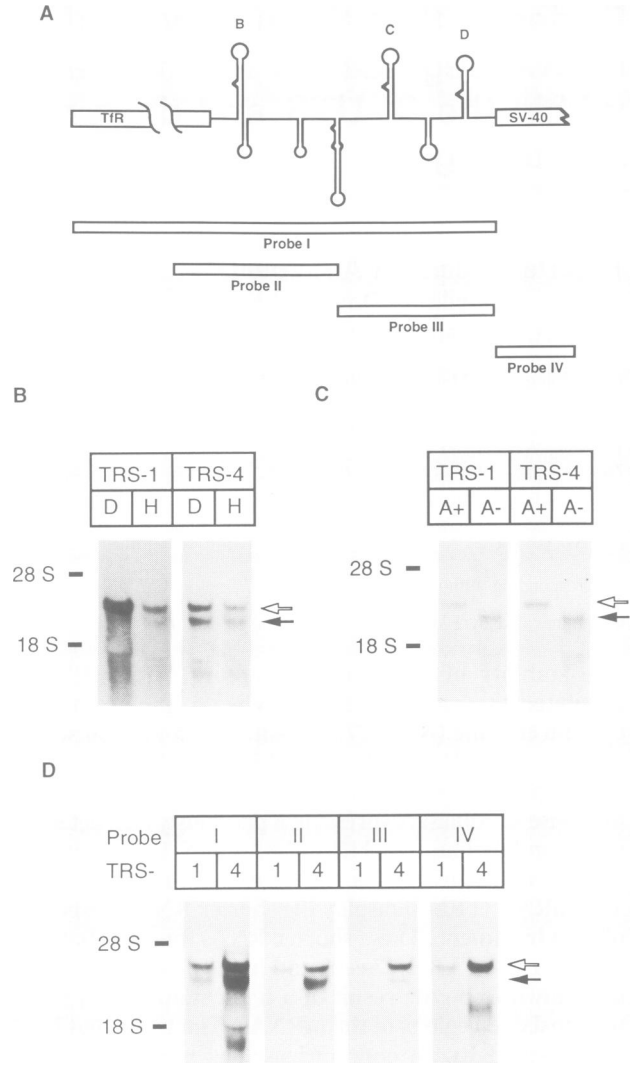

Fig. 2. TRS-1 and TRS-4 mRNA from B6 fibroblasts exhibits a shorter RNA that lacks a portion of the 3′ UTR. (**A**) Shown are the hybridization probes used in panels B, C and D. All probes were produced by random priming restriction fragments of plasmid TRS-1 in the presence of [α-^{32}P]dCTP. Probe I, a 2629 nt fragment beginning at an *Eco*RV site (nt 14 of TfR mRNA, numbered as described in Casey *et al.*, 1988b); Probe II, a 727 nt fragment beginning at a *Sty*I site (nt 1777 of TfR mRNA); Probe III, a 137 nt fragment beginning at an *Xho*I site (nt 3663 of TfR mRNA); Probe IV, a 242 nt fragment beginning at a *Bam*HI site [corresponding to nt 2533 in SV40 (Buchman *et al.*, 1980)]. The TfR coding region and the SV-40 polyadenylation region are indicated. (**B**) The stably transfected cell lines TRS-1 and TRS-4 were treated for 17 h with 6 mM sodium butyrate and either 100 μM hemin or 100 μM desferrioxamine. RNA (10 μg) was electrophoresed through a vertical 1.2% agarose−2.2 M formaldehyde gel (VAGE, Stratagene) and pressure-blotted to nytran. The blot was hybridized with probe I as described in Figure 1A. Full-length mRNAs and truncated RNA are indicated by an open arrow and a solid arrow, respectively. (**C**) RNA from TRS-1 and TRS-4 cells treated with hemin as described in panel B was subjected to oligo(dT) cellulose chromatography. Poly(A)$^-$ RNA (10 μg) and its poly(A)$^+$ RNA counterpart were electrophoresed, blotted and hybridized with Probe I as described in panel B. Full-length mRNAs and truncated RNAs are indicated by an open arrow and a solid arrow, respectively. (**D**) RNA (10 μg) from TRS-1 and TRS-4 cells treated with hemin was electrophoresed in quadruplicate and blotted as described in panel B. The four blots were separately hybridized with the indicated probes. Full-length mRNAs and truncated RNAs are indicated by an open arrow and a solid arrow, respectively.

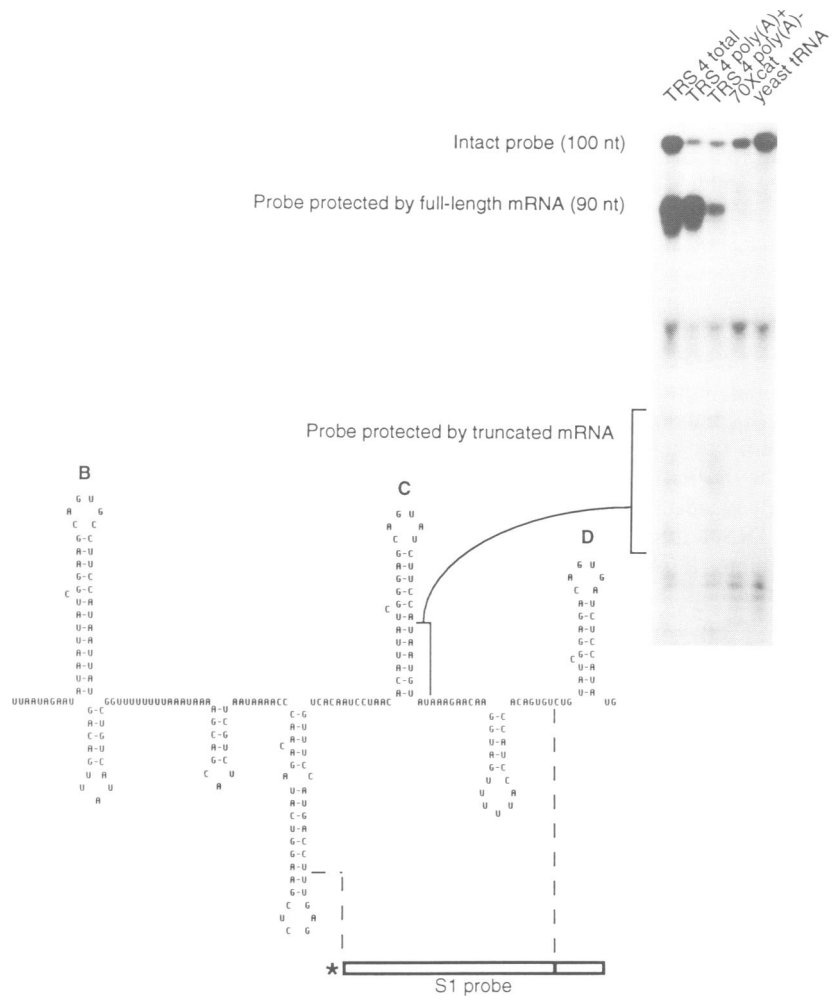

Fig. 3. S1 nuclease protection maps the 3′ end of the truncated TRS-4 RNA to single-nucleotide resolution. RNA (150 μg) from TRS-4 cells treated with sodium butyrate (6 mM; 15 h) was fractionated with oligo(dT) cellulose chromatography into the poly(A)$^+$ and poly(A)$^-$ fractions. These RNA samples, together with RNA from unfractionated TRS-4 cells, from 70XCAT cells [a stable cell line of B6 fibroblasts that expresses a non-TfR-containing plasmid (plasmid 70XCAT described in Casey *et al.*, 1988a)], and yeast tRNA were annealed with 1×10^5 c.p.m. of the S1 probe, as described in Materials and methods. Unprotected probe was digested with 1000 U/ml of S1 nuclease. Reaction products were electrophoresed through a 6% polyacrylamide sequencing gel. Intact probe and S1 resistant products reflecting full-length and truncated RNAs are indicated on the autoradiogram. The positions of the S1 probe and the S1 nuclease resistant products reflecting truncated mRNA are shown schematically on the TRS-1 mRNA secondary structure model of Horowitz and Harford (1992). The probe was 3′ end-labeled (*) and the shaded portion of the probe is not complementary to the TRS-4 mRNA.

shorter RNA lacked a poly(A) tail, as indicated by its failure to be retained by an oligo(dT) column (Figure 1B). However, the large reduction in size suggested that more than the poly(A) tail was missing from the shorter RNA. This suggestion was confirmed by assessing hybridization of the shorter RNA with probes specific for selected regions of the TfR mRNA 3′ UTR. The shorter RNA hybridized to two probes complementary to nt 2955−3631, and nt 3598−3856, respectively but failed to hybridize to a probe complementary to nt 3856−4340 (data not shown). This result indicated that the shorter RNA is missing all or most of the sequence corresponding to the 3′-most probe. The non-hybridizing probe corresponds to sequences just 3′ of the 678 nt region previously mapped as being critical to TfR mRNA regulation by iron (Casey *et al.*, 1988b) indicating that the truncation of the mRNA is occurring within or near this critical regulatory region.

We have previously reported that as little as 250 nt can confer iron regulation upon an mRNA encoding the human TfR (Casey *et al.*, 1989) in stable transformants of murine B6 fibroblasts. The 3′ UTR of the plasmid TRS-1, consists of a 250 nt fragment of the TfR 3′ UTR cloned 12 nt downstream of the translation stop codon of the TfR protein. The TRS-1 cassette consists of nt 3285−3389 plus nt 3663−3788 of the human TfR mRNA separated by an exogenous *Xho*I site used in the construction (Casey *et al.*, 1989). The 250 nt fragment of TRS-1 contains three iron-responsive elements termed B, C and D, and thereby confers iron regulation to mRNA degradation. The TRS-1 regulatory cassette is followed immediately by an SV40 early polyadenylation signal (Figure 2A). The related plasmid TRS-4 is identical except that it lacks three C residues corresponding to the most 5′ C of each of the three IRE loops. The elimination of this C from an IRE markedly reduces the affinity of interaction with the IRE-BP (Casey *et al.*, 1989; Haile *et al.*, 1989; Jaffrey *et al.*, 1993). Whereas the stability of TRS-1 mRNA is regulated by iron, TRS-4 mRNA is constitutively unstable (Casey *et al.*, 1989;

Koeller *et al.*, 1991). When TRS-1 cells are treated with hemin, a shorter RNA is apparent, analogous to the situation seen with ARH-77 cells (Figure 2B, left panel). In contrast, mRNA preparations from TRS-4 cells contain the shorter RNA irrespective of iron treatment (Figure 2B, right panel). In a related cell line expressing a human TfR mRNA termed TRS-3 that is constitutively stable (Casey *et al.*, 1989; Koeller *et al.*, 1991) no shorter mRNA is observed under any iron treatment regimen (data not shown). The conclusion that the shorter RNAs are intermediates in mRNA decay is supported by: (i) the iron-dependent appearance of a shorter RNA in TRS-1 wherein the human TfR mRNA is iron-regulated; (ii) the constitutive presence of the shorter RNA in TRS-4 cells wherein the human TfR mRNA is constitutively unstable; and (iii) the absence of the shorter RNA in TRS-3 cells wherein the human TfR mRNA is always stable. The fact that the shorter RNAs in TRS-1 cells and TRS-4 cells are apparently identical in size indicates that the constitutively unstable TRS-4 mRNA is likely being degraded by a pathway similar, if not identical, to that operative on TRS-1 mRNA in hemin-treated cells.

The shorter human TfR RNAs in TRS-1 and TRS-4 cells resembled the shorter RNA in ARH-77 cells in that they were not retained by an oligo(dT) column (Figure 2C). These results suggested that the shorter RNAs in the mouse fibroblasts were likely truncated within their 3′ UTR in analogy to the endogenous TfR mRNA of ARH-77 cells. This suggestion was confirmed by hybridization with a series of probes that span the 3′ UTRs of the TRS-1 and TRS-4 mRNAs (Figure 2A). The relative hybridization signals of the shorter RNAs (compared with the full-length mRNA) were markedly decreased with probe III and absent with probe IV (Figure 2D). These findings demonstrated that the 3′ ends of the truncated RNAs are within the region covered by probe III. These data indicated that the truncation is occurring within the IRE-containing 250 nt cassettes of both the TRS-1 and TRS-4 mRNAs. Although the 3′ UTR of the TRS-1 mRNA is only about one-tenth the size of that of native human TfR mRNA, the similar characteristics of the truncated RNAs in both cases suggests that both the native TfR mRNA and the TRS mRNAs are being degraded by similar pathways.

More precise mapping of the 3′ end of the truncated RNA in TRS-4 cells was achieved by S1 nuclease protection (Figure 3). Based on the above findings indicating that the 3′ end was within probe III, an S1 probe was designed that was complementary to 90 nt of TRS-4 mRNA starting just 5′ of IRE C and extending to a point just 5′ of IRE D. The probe contained 10 nt unrelated to the TfR mRNA at its 5′ end and was 3′ end-labeled as described in Materials and methods. The unrelated nucleotides enabled the distinction between probe protected by full-length TRS-4 mRNA and undigested probe. In addition to the band arising from protection by full-length TRS-4 mRNA, a series of shorter protected fragments were observed. These shorter probe fragments are not generated from the full-length mRNA since they are absent in the poly(A)$^+$ RNA where the full-length mRNA is found. Instead, the shorter fragments are found in the poly(A)$^-$ RNA that had been shown in Figure 2C above to contain the truncated TRS-4 RNA. The shorter protected probe fragments correspond to truncations of the TRS-4 mRNA on the 3′ side of the bottom of IRE C, a location contained within probe III of Figure 2A. It would

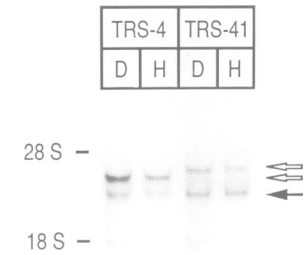

Fig. 4. Northern analysis of TRS-4 and TRS-41 mRNA. RNA samples (10 μg) from TRS-4 and TRS-41 cells treated with either hemin (H) or desferrrioxamine (D) were electrophoresed, blotted and hybridized as described in Figure 2B. Full-length and truncated RNAs are indicated by open arrows and a solid arrow, respectively. Note that the full-length mRNA from TRS-41 cells is ~250 nt longer than that from TRS-4 cells whereas the truncated RNAs appear identical in size.

appear from the pattern of protected fragments that there is more than one 3′ end of the truncated RNA. However, this pattern could be generated either from a frayed 3′ end of the target RNA or from 'breathing' of the probe-RNA hybrid allowing 'nibbling' of the radiolabeled probe during the S1 nuclease digestion.

The truncated TfR RNAs might arise either from a pathway involving an endonucleolytic cleavage or from a pause in the progressive digestion by a 3′→5′ exonuclease. To begin to address this issue, a new chimeric construct termed TRS-41 was prepared in which the 250 nt regulatory cassette of TRS-1 was placed immediately 3′ of the 250 nt TRS-4 element that conferred constitutive instability. Thus, TRS-41 mRNA is ~250 nt larger than either TRS-1 or TRS-4 mRNAs. It was anticipated that if the TRS-4 element were a constitutive endonuclease target site, it should act in a dominant fashion to confer instability of the TfR mRNA made from TRS-41 irrespective of iron. If instead the mRNA were degraded by a 3′→5′ exonuclease, then the 3′-most cassette from TRS-1 might be expected to impede the appearance of the truncated mRNA at least in chelator-treated cells wherein the TRS-1 IREs would be engaged by the IRE-BP. Northern blot analysis confirmed that the TRS-41 mRNA is not regulated by iron and that it is truncated within the region corresponding to the TRS-4 element (Figure 4). A time-course of TRS-41 mRNA decay in the presence of actinomycin D confirmed that this mRNA is equally unstable in the presence or absence of iron (data not shown). Thus the presence of a functional regulatory cassette from TRS-1 3′ of the truncation site was not sufficient to confer iron dependence to the stability of TRS-41 mRNA. This result is most consistent with an endonucleolytic cleavage within the TRS-4 cassette of TRS-41 mRNA. The fact that a single shorter RNA is observed in TRS-41 cells even in hemin suggests that the 5′-most element is the preferred cleavage site even when two such sites are theoretically available. It is also possible that the product of the cleavage within the TRS-1 element of TRS-41 mRNA is itself highly unstable and is not detected in these experiments.

By far the best evidence for an endonuclease mechanism in the generation of the truncated TfR RNAs would be to detect the corresponding 3′ fragment that would be produced. A 3′→5′ exonuclease would not generate such a fragment. Primer extension analyses were performed using a 5′ end-

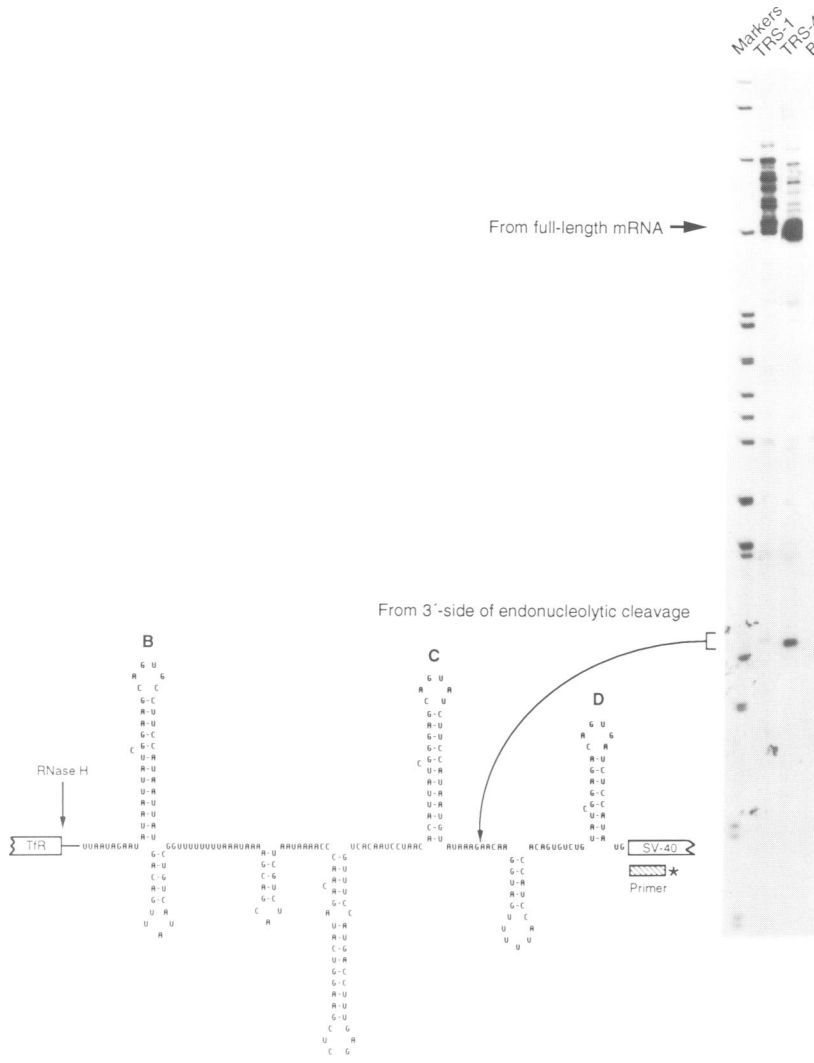

Fig. 5. Primer extension detects the 3′-fragment that results from an endonuclease cleavage of TRS-1 and TRS-4 mRNAs. TRS-1 and TRS-4 RNA samples (50 and 25 μg, respectively) from cells that were desferrioxamine-treated as described in Figure 2B were first cleaved near the translation stop codon using antisense oligonucleotide-directed RNase H cleavage, as indicated on the secondary structure model and described in Materials and methods. The RNase H-cleaved RNA samples were analyzed by primer extension with 2×10^5 c.p.m. of the 5′ end-labeled antisense oligonucleotide indicated and described in Materials and methods. The bands arising from the full-length mRNA and from the 3′ endonucleolytic cleavage fragment are indicated on the autoradiogram. The location of the cleavage site is indicated on the secondary structure model. RNA (25 μg) from untransfected B6 fibroblasts was subjected to identical RNase H treatment and primer extension. Markers shown are pBR322 DNA cut with the restriction enzyme *Msp*I.

labeled oligonucleotide complementary to part of the SV40 polyadenylation region (see Figure 5 schematic). Prior to the annealing and extension reactions, the target TfR mRNA was cleaved near the translation stop codon using oligonucleotide-directed RNase H cleavage. As a result of the RNase H cleavage, the primer extension fragment generated from the full-length mRNAs would be short enough to resolve on a 6% polyacrylamide sequencing gel. Using mRNA preparations from chelator-treated TRS-1 and TRS-4 cells, a shorter primer extension product was detected. Based on comparison with a dideoxy sequencing ladder (not shown), it was concluded that this extension product corresponds to an RNA having nt 3728 of the human TfR mRNA as its 5′ end (Figure 5). As would be expected, this fragment is much more abundant relative to the full-length primer extension product in TRS-4 mRNA than in the TRS-1 mRNA. Other primer extension products observed may correspond to reverse transcriptase pause sites since they are equally abundant in TRS-1 and TRS-4 mRNAs. The major site mapped by primer extension is very near the nucleotides mapped by S1 protection in Figure 3, as would be expected if the two fragments were the two matching RNA products generated by the action of an endonuclease. To confirm that the primary primer extension product is a cDNA synthesized from an endonuclease fragment of TRS-4 mRNA and not simply a pause site for reverse transcriptase on full-length mRNA, TRS-4 RNA was size-fractionated by sucrose gradient sedimentation prior to primer extension analysis (Figure 6). Using this method, the 3′ fragment (peaking in fraction 2) was clearly resolved from the full-length mRNA (peaking in fraction 4). Thus, the signal in the primer extension assay arises from an RNA considerably smaller than the full-length TRS-4 mRNA.

All of the above observations are consistent with an endonucleolytic cleavage at a site between a G and an A residue corresponding to nt 3727 and 3728 of the human

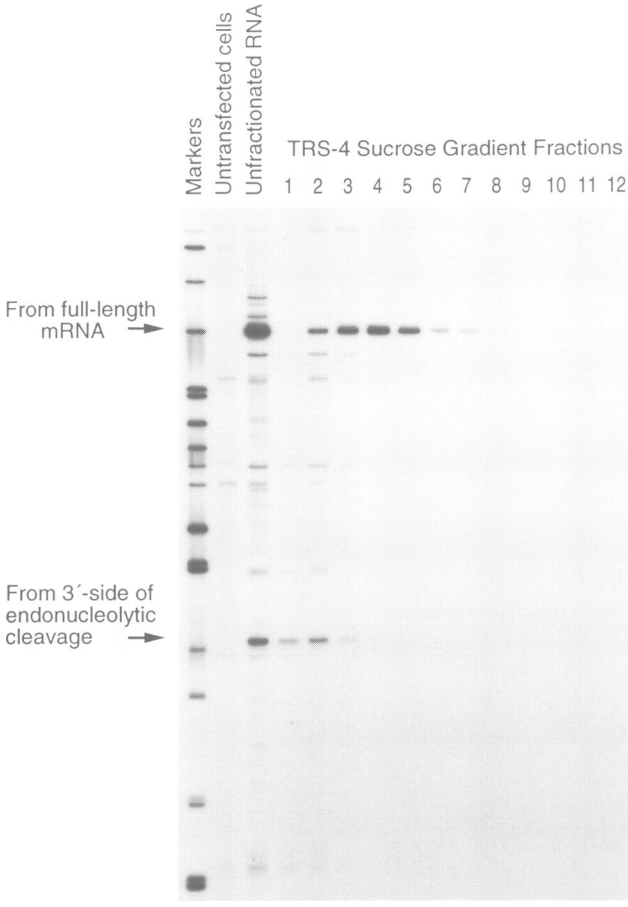

Fig. 6. Sucrose gradient size fractionation separates full-length TRS-4 mRNA from the 3′ endonuclease cleavage fragment. RNA (100 μg) from TRS-4 cells treated with sodium butyrate (6 mM; 16 h) was subjected to size fractionation by sucrose gradient sedimentation as described in Materials and methods. The RNA from each gradient fraction was analyzed by primer extension as described in Figure 5. The lanes to the left of the gradient fractions represent (from left to right) radiolabeled markers (*Msp*I-cut pBR322 DNA), primer extension products from RNA (50 μg) of untransfected B-6 cells, and primer extension of unfractionated TRS-4 RNA (50 μg).

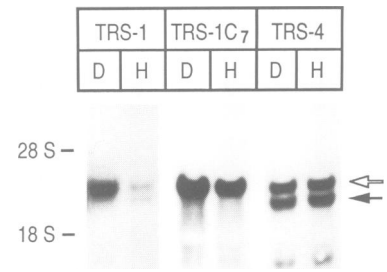

Fig. 7. TRS-$1C_7$ mRNA exhibits reduced iron regulation and no truncated degradation intermediate. RNA (10 μg) from TRS-1, TRS-$1C_7$ and TRS-4 cells treated with either desferrioxamine (D) or hemin (H) was electrophoresed, blotted and hybridized as described in Figure 2B. Full-length mRNAs and truncated RNAs are indicated by an open arrow and a solid arrow, respectively. Note that the regulation seen in TRS-1 cells and the shorter RNA seen in TRS-1 and TRS-4 cells are absent in TRS-$1C_7$ cells.

TfR mRNA, respectively. This site falls within a region of the mRNA that has been shown to be single-stranded in TRS-1 RNA (Horowitz and Harford, 1992). Although relatively AU-rich, the nucleotide sequence of this region does not contain the AUUUA sequence that has been implicated in the turnover of other mRNAs (Shaw and Kamen, 1986). Indeed, the AUUUA motif is absent altogether in the TRS cassettes. An endonucleolytic cleavage of the mapped region of the TfR mRNA might be sequence-specific or might be directed by surrounding RNA structure without regard to the nucleotide sequence immediately surrounding the cleavage site. To address this question, a 7 nt segment of TRS-1 (nt 3727−3733 of the TfR mRNA) containing the mapped cleavage site was changed from the sequence GAACAAG to a homopolymeric stretch of Cs. This construct, TRS-$1C_7$, was stably expressed in mouse B6 fibroblasts and the iron regulation of the resulting mRNA was compared with that of TRS-1 and TRS-4. The change of sequence resulted in a marked reduction in the regulation of the mRNA by iron (Figure 7). Furthermore, no truncated TRS-$1C_7$ mRNA was observed under any iron treatment regimen, indicating that TRS-$1C_7$ mRNA is not a substrate for the endonuclease that normally targets TfR mRNA. This result suggests that the endonuclease involved in cleavage at this site has some degree of sequence specificity. It is of note that the sequence of this region is identical in human and chicken TfR mRNAs (Koeller *et al.*, 1989) and also in rat TfR mRNA (Roberts and Griswold, 1990). However, it should also be noted that there exists extensive sequence similarity throughout the 250 nt TRS-1 regulatory region. Moreover, certain other sequence elements within the region corresponding to TRS-1 have also been shown to be critical for iron regulation of mRNA stability (Casey *et al.*, 1989).

There is a growing body of evidence suggesting that poly(A) tail shortening precedes the degradation of several short-lived mRNAs and it has been suggested that such poly(A) shortening is a prerequisite for the turnover of these mRNAs (Bernstein and Ross, 1989; Sachs, 1990; Baker 1993; Rubin and Halim, 1993). The relationship between poly(A) tail removal and mRNA degradation is largely based on the kinetics of the two processes and the fact that certain inhibitors (e.g. cycloheximide) block both processes (Laird-Offringa *et al.*, 1990). Our findings indicating an endonucleolytic cleavage within the 3′ UTR of the TfR mRNA and the fact that we have detected both products of the cleavage reaction allows us to assess the state of the poly(A) tail of this mRNA both before and after the cleavage step. The poly(A) tails on full-length mRNA were measured by the method described by Brewer and Ross (1988). Endogenous TfR mRNA from ARH-77 cells that had been treated with hemin for 0−4 h, was cleaved at a site close to the poly(A) tail using oligonucleotide-directed RNase H cleavage and the 3′ product containing the poly(A) tail sized by Northern blot analysis using a probe complementary to sequence between the RNase H cleavage and the poly(A) tail (Figure 8A). As the overall signal intensity decreased during the time-course of hemin treatment, there was no significant qualitative change in the apparent length of the poly(A) tail. This observation is in contrast to the aforementioned observations with other short-lived mRNAs where a similar experimental protocol detects poly(A) tail shortening. Poly(A) tail length was also measured in TRS-1 and TRS-4 mRNA from chelator-treated cells (Figure 8B). Under these conditions, TRS-4 mRNA is unstable and TRS-1 mRNA is stable. Despite their different stabilities, both mRNAs have a similar poly(A) tail length. This type of

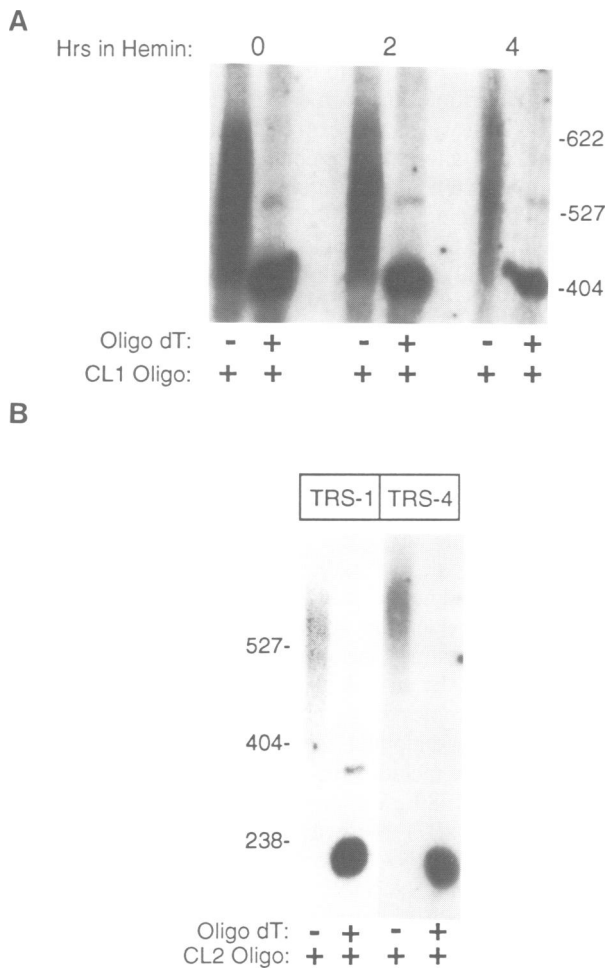

Fig. 8. Poly(A) tail length is not significantly altered during rapid degradation of TfR mRNAs. (**A**) ARH-77 cells (9.4×10^5 cells/ml) were treated with hemin (100 μM) for the times indicated. RNA was isolated from 50 ml of cells at each time point and subjected to antisense oligonucleotide-directed RNase H cleavage with either CL1 oligonucleotide alone [which generates a heterogeneous band reflecting the different poly(A) tail lengths in the population of TfR mRNAs] or CL1 plus oligo(dT) [which generates a single band reflecting the deadenylated TfR mRNA fragment that lies between the CL1 cleavage site and the poly(A) tail]. Samples were subjected to Northern blot analysis as described in Materials and methods. At all time points, surviving TfR mRNA has a similar distribution of poly(A) lengths. (**B**) TRS-1 and TRS-4 cells (at 50% confluency) were treated with desferrioxamine as described in Figure 2B. RNA (5 μg) was subjected to antisense oligonucleotide-directed RNase H cleavage with either CL2 oligonucleotide alone or CL2 plus oligo(dT). Samples were analyzed as described in panel A. The poly(A) tails on the relatively unstable TRS-4 mRNA and on the relatively stable TRS-1 mRNA appear to have comparable length distributions.

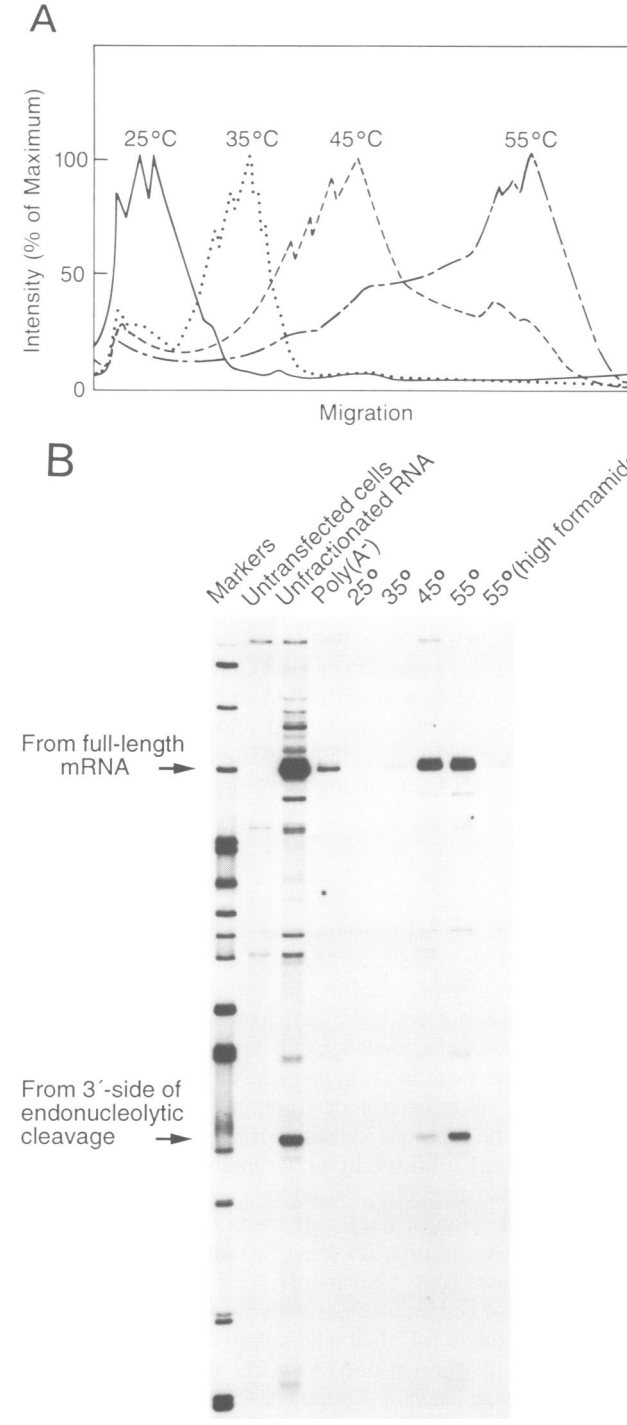

Fig. 9. The poly(A) tail on the 3′ endonucleolytic cleavage product is indistinguishable from that of the full-length TfR mRNA. RNA (100 μg) from TRS-4 cells treated with sodium butyrate (6 mM; 21 h) was fractionated according to poly(A) tail length by temperature elution from poly(U)−Sephadex, as described in Materials and methods. (**A**) Ten percent of each fraction was 3′ end-labeled with [^{32}P]pCp, digested with RNase A and RNase T1 to digest the body of the mRNA and the resultant radiolabeled poly(A) tails resolved on a 6% polyacrylamide gel. Each lane of this gel was scanned for radioactivity using a Molecular Dynamics Phosphorimager. The gel migration patterns of the RNA eluting from the poly(U)−Sephadex column at the indicated temperatures are shown with the left being the bottom of the sequencing gel [smaller poly(A) tails]. (**B**) Fifty percent of each fraction together with unfractionated TRS-4 RNA (50 μg) and RNA from untransfected B6 fibroblasts (50 μg) were primer extended as in Figure 5. Markers shown are pBR322 DNA cut with the restriction enzyme *Msp*I.

experimental protocol only looks at surviving full-length mRNA. If a very rapid degradation of the body of the mRNA follows poly(A) tail shortening, it is conceivable that it might be difficult to detect the small amount of mRNA on which the poly(A) tail had been shortened. In other words, the inability to detect full-length TfR mRNA with a shortened poly(A) tail could conceivably be the result of a very rapid flux through the degradation intermediate having only its poly(A) tail shortened.

To address this issue, we assessed the state of the poly(A) tail on the 3′ cleavage product detected by primer extension in Figure 5. If this cleavage fragment had a poly(A) tail of

the same length as the full-length mRNA, then no poly(A) tail shortening preceded the endonucleolytic cleavage that generated the fragment. Temperature elution of RNA that was bound to poly(U)−Sephadex was performed in order to compare the length of the poly(A) tail of the 3′ fragment and the full-length mRNA. The ability of the poly(U)−Sephadex to fractionate cellular RNAs on the basis of poly(A) tail length was first confirmed by 3′ end-labeling each of the fractions from the temperature elution followed by digestion of the labeled RNA with RNase A and T1 to destroy all but the radiolabeled poly(A) tails, which were resolved on a 6% polyacrylamide sequencing gel. With progressively higher temperatures of elution from poly(U)−Sephadex, the average size of the radiolabeled poly(A) tails increased indicating that this protocol was indeed sensitive to poly(A) tail length (Figure 9A). The TfR full-length mRNA and 3′ fragment were each visualized by primer extension analysis (Figure 9B). The full-length mRNA and the 3′ fragment displayed the same elution profile, indicating that they are both polyadenylated to the same extent with >95% of each RNA eluting from poly(U)−Sephadex at 45 and 55°C. Taken together with the measurement of poly(A) tail length on the endogenous TfR mRNA during iron-stimulated degradation (Figure 8A) and the similarity in poly(A) tail length on a stable and unstable TRS mRNA (Figure 8B), these data are most consistent with the degradation of TfR mRNAs involving no prior change in poly(A) tail length.

Discussion

Although some *cis*-acting sequences, cellular components and processes have been identified as playing a role in the regulation of mRNA stability, a complete pathway for degradation has not yet been described for any eukaryotic mRNA. Our lack of knowledge concerning the mechanisms of mRNA turnover reflects, in part, the difficulty in detecting intermediates in transcript destruction. This difficulty is thought to be the consequence of the primary event in mRNA breakdown being followed by very rapid degradation of the products of that triggering reaction.

The identification of intermediates in the degradation of a given mRNA can provide some insight as to what types of ribonucleases may be involved. For example, the accumulation of certain mRNAs with shortened poly(A) tails during the course of their degradation have suggested ribonucleases that target poly(A) (Greenberg and Belasco, 1993). In yeast, such a ribonuclease, termed PAN [for poly(A) nuclease], has been characterized and cloned (Sachs and Deardorff, 1992). The poly(A) tail has long been suggested to play a role in mRNA stability (for reviews see Bernstein and Ross, 1989; Sachs, 1990; Baker, 1993; Rubin and Halim, 1993). One model for poly(A) tail involvement in mRNA degradation envisions the shortening of the poly(A) tail to some critical length triggering the further degradation of the mRNA (by mechanisms that remain obscure). This model is supported (but not proven) by experiments demonstrating that both shortening of the poly(A) tail of c-*myc* mRNA and degradation of the c-*myc* transcript are inhibited by cycloheximide (Laird-Offringa *et al.*, 1990).

Insight into the pathway of mRNA decay can be gained from a characterization of breakdown intermediates. Unfortunately, such intermediates are rare. A short form (2.7 kb) of the TfR mRNA has previously been reported in mouse plasmacytoma cells (Neckers *et al.*, 1986). This RNA species was shown to differ from the full-length TfR mRNA by virtue of the former lacking at least a portion of the 3′ UTR. It was not determined whether this RNA arose as a result of alternative splicing, alternative poly(A) site selection or enzymatic truncation. For some other eukaryotic mRNAs including those encoding c-*myc* and c-*fos* (Laird-Offringa *et al.*, 1990), chick fibroblast 9E3 (Stoeckle and Hanafusa, 1989), chicken apo VLDL II (Binder *et al.*, 1989), human gro-α (Stoeckle, 1992), yeast PGK1 (Vreken and Raué, 1992), *Xenopus Xlhbox2B*, (Brown and Harland, 1990) and human histone H4 (Ross *et al.*, 1986), RNA fragments with truncated 3′ ends have been detected. Such fragments might result from specific endonucleolytic cleavage or a defined pause site in the processive action of a 3′→5′ exonuclease. For most of the above cited RNA fragments, their 3′ ends have not been determined with precision and the enzymes responsible for their production remain unknown. For human IGF II mRNA (Meinsma *et al.*, 1991) and human β-globin mRNA (Lim *et al.*, 1992), degradation products that are missing their 5′ ends have been detected suggesting that these truncated mRNAs are generated either by an endonuclease or a 5′→3′ exonuclease.

In a few examples the two matching fragments that would result from an endonuclease cleavage *in vivo* have been detected. These include chicken liver apo VLDL II mRNA (Binder *et al.*, 1989), *Xenopus* oocyte *Xlhbox2B* mRNA (also known as HoxB7) (Brown and Harland, 1990), chick fibroblast 9E3 mRNA (Stoeckle and Hanafusa, 1989) and yeast *PGK1* mRNA (Vreken and Raué, 1992). These breakdown products have not been fully characterized.

Our data support a model for TfR mRNA breakdown that involves an endonucleolytic cleavage of the mRNA. We first detected in a human plasmacytoma cell line, a shorter RNA that lacks a significant portion of the 3′ end of the TfR mRNA (Figure 1). Truncated RNAs are also seen in mouse fibroblasts expressing human TfR mRNAs (Figure 2). The 3′ end of the truncated mRNA has been mapped to a region of the mRNA just downstream of IRE C (Figure 3). The appearance of the truncated TfR RNAs correlated with rapid turnover of the TfR mRNA. In ARH77 cells (Figure 1) and in mouse cells expressing the iron-regulated construct TRS-1 (Figure 2), the truncated RNAs were seen only upon iron treatment of the cells. In mouse cells expressing the constitutively unstable TRS-4 construct, the truncated RNA was present irrespective of the iron status of the cells (Figure 2). In mouse cells expressing the unregulated TRS-3 construct, the truncated RNA was never seen regardless of iron treatment (data not shown). All of these data are consistent with the shorter RNAs being intermediates in the breakdown of the TfR transcripts.

We prepared a construct called TRS-41 in which the cassette corresponding to the regulatory region of TRS-1 was placed immediately downstream of the TRS-4 cassette that confers constitutive instability. The resultant mRNA was 250 nt longer than TRS-4, but an apparently identical truncated RNA was present even upon treatment of the TRS-41 cells with desferrioxamine (Figure 4). In desferrioxamine-treated cells, the IRE-BP is active and would be expected to bind to the IREs within the downstream TRS-1 cassette of TRS-41 mRNA. This binding of the IRE-BP would, in turn, be expected to prevent a putative 3′→5′ exonuclease from

reaching the truncation site within the TRS-4 cassette. In contrast, an endonuclease might be expected to attack the TRS-4 cassette of TRS-41 mRNA without regard to the association of the IRE-BP with the downstream TRS-1 cassette and thereby give rise to a truncated RNA identical to that seen in TRS-4. The latter is indeed observed. Thus, this result suggested that the truncated RNA was the result of an endonucleolytic cleavage rather than a 3′→5′ exonuclease pause. The TRS-41 mRNA was shown to be short-lived irrespective of iron by an experiment examining decay of the mRNA in the presence of actinomycin D (not shown). Interestingly in TRS-41 cells treated with hemin, there does not appear to be a truncated mRNA corresponding to a cleavage within the TRS-1 cassette. This finding implies that the 5′-most cleavage within the TRS-4 cassette is highly favored or that the product of a cleavage within the TRS-1 cassette is very unstable.

The endonucleolytic nature of the process that generates the truncated RNA in TRS-4 cells was confirmed by detection of the corresponding downstream fragment (Figure 5). Whereas the 3′ end of the upstream fragment appeared to be frayed based on the S1 protection assay (Figure 3), the 5′ end of the downstream fragment detected by primer extension mapped to a single nucleotide within a single stranded region just 3′ of IRE C. We demonstrated that the primer extension product was not the result of a pause during reverse transcription of the full-length mRNA by showing that the RNA giving rise to this fragment could be separated from full-length mRNA by sucrose gradient centrifugation (Figure 6). The mRNA scission we detected occurred just 3′ of a G residue within a segment of the TfR mRNA that is very AU-rich (Figure 5). Although the TRS-1 cassette as a whole is AU-rich, it does not contain the AUUUA motif implicated in turnover of other mRNAs (Shaw and Kamen, 1986). The TfR mRNA segment mapped here as an endonuclease cleavage site has a sequence that is identical to those of the corresponding portions of the rat (Roberts and Griswold, 1990) and chicken (Koeller *et al.*, 1989) TfR mRNAs. In human TRS-1 mRNA, this region has been demonstrated to be single-stranded having double-stranded segments on either side of it (Horowitz and Harford, 1992). Endonucleolytic cleavage of chicken apo VLDL II mRNA also occurs within single-stranded regions of a rather complex RNA secondary structure (Binder *et al.*, 1989).

To begin to address the issue of the specificity of the endonuclease responsible for the cleavage that we had detected, a 7 nt segment (GAACAAG) containing the mapped cleavage site was replaced with an equivalent number of C residues. This change of sequence resulted in a loss of the truncated RNA and an abrogation of iron regulation of the level of TfR mRNA (Figure 7). In previous work from this laboratory, certain deletions within the regulatory region also resulted in a loss of iron regulation of mRNA stability indicating that these segments are also critical, in one way or another, to mRNA degradation (Casey *et al.*, 1989). Within the native TfR mRNA, one such critical region resides some 300 nt upstream of the cleavage site that we have mapped here. One possible explanation for these findings is that the rapid turnover determinant of the TfR mRNA is a relatively complex structure in three-dimensional space. Primary or secondary sequence/structure elements that are distant in the primary sequence may be brought into proximity by RNA folding. Together they may form the recognition determinant for the cellular machinery of degradation. It is also conceivable that the critical elements implicated by the deletion analyses are not themselves directly part of the recognition determinant, but rather are distant structural elements whose deletion perturbs the overall geometry of the recognition determinant. If this were the case, they would be analogous to amino acids that are not part of the active site of an enzyme but whose removal abolishes enzymatic activity through an overall conformational change in the protein. While a detailed analysis of the sequence requirements for cleavage remains to be done, our results suggest that the endonuclease that generates the fragments described here has some degree of sequence specificity.

We also addressed the question of whether poly(A) tail shortening occurs in the course of TfR mRNA degradation, as has been reported for a number of mRNAs. RNA was isolated from ARH-77 cells during a hemin time-course and the length of the TfR mRNA poly(A) tail assessed using the methodology of Brewer and Ross (1988). No significant difference in poly(A) tail length was noted even though >50% reduction occurred in the level of TfR mRNA (Figure 8A). A similar analysis was also performed on RNA isolated from TRS-1 and TRS-4 cells treated with desferrioxamine. Under these conditions, the TRS-1 mRNA is relatively stable whereas the TRS-4 mRNA is relatively unstable. Despite differences in stability, the TRS-1 and TRS-4 mRNAs appear to have comparable distributions of poly(A) tail length with the mean length appearing to be ~300 nt (Figure 8B).

A difficulty with experiments like those described in Figure 8 is that the mRNA that is examined is the surviving population of transcripts. If very rapid degradation occurs following poly(A) shortening, then the level of mRNA having a shortened poly(A) tail could be missed in an analysis of this type. Our ability to detect the downstream product of the endonucleolytic cleavage enabled us to address the question of whether poly(A) tail shortening had preceded the cleavage. The RNA giving rise to the primer extension product characteristic of the 3′ side of the cleavage was retained by an oligo(dT) column. The minimal length of poly(A) tail that is retained by an oligo(dT) column ranges from 10 to 30 residues (Littauer and Soreq, 1982) meaning that the poly(A) tail on the downstream fragment could have been shortened considerably and still be retained by the column. Poly(U)−Sephadex can retain RNAs with as few as 6−10 A residues and RNAs with different length poly(A) tails can be differentially eluted from such a column (Rosenthal *et al.*, 1983). Therefore, we compared the poly(U)−Sephadex temperature elution profile of the full-length TRS-4 mRNA with that of the downstream fragment. Having established that bulk RNA was differentially eluted using this protocol based on poly(A) tail length, we found that the poly(A) tail of the downstream fragment was comparable in length with that of the intact TRS-4 mRNA. These results strongly suggest that the endonucleolytic cleavage of the TfR mRNA occurs without prior shortening of the poly(A) tail. In the case of chick fibroblast 9E3 mRNA, available evidence also indicates that prior deadenylation is not a requirement for the cleavage reaction (Stoeckle and Hanafusa, 1989). In contrast, it was shown that PGK1 mRNA loses its poly(A) tail prior to the endonuclease cleavage event (Vreken and Raué, 1992).

Clearly, eukaryotes possess a variety of ways by which controlled mRNA degradation can be achieved.

We have previously proposed that the destabilization by iron of TfR mRNA was the result of an iron-dependent inactivation of the IRE-BP (Casey *et al.*, 1989; Koeller *et al.*, 1989). This model envisions the rapid turnover determinant of the mRNA and the binding site for the IRE-BP as being near or overlapping with each other. The association of the IRE-BP with the mRNA apparently results in protection of the mRNA against nucleolytic attack. The finding of a specific endonucleolytic cleavage site near one of the IREs is certainly consistent with this model. A similar model has recently been proposed for the *Xlhbox 2B* mRNA and *Xoo1* mRNA of *Xenopus* (Brown *et al.*, 1993). A number of other *trans*-acting cytoplasmic RNA binding proteins have been implicated in the control of stability of mRNAs *in vivo* (Schuler and Cole, 1988; Malter, 1989; Stern *et al.*, 1989; Weber *et al.*, 1989; Bohjanen *et al.*, 1991; Brewer, 1991; Liang and Jost, 1991; Vakalopoulou *et al.*, 1991; Bernstein *et al.*, 1992; Myer *et al.*, 1992; You *et al.*, 1992). In some cases the protein appears to be essential for the nuclease activity rather than acting as a protector like the IRE-BP. For example, yeast PAN requires the poly(A) binding protein for activity (Sachs and Davis, 1989). It appears that the interaction with mRNA by distinct RNA binding proteins can have opposite effects on mRNA stability with some acting to stabilize while others destabilize (Lowell *et al.*, 1992).

The iron-regulated turnover of the TfR mRNA is one of the better understood systems of mRNA decay in higher eukaryotes. The regulatory region has been mapped as having binding sites for a cloned RNA binding protein (i.e. the IRE-BP) that serves to protect the mRNA from decay. We now have some evidence suggesting that a sequence-specific endonuclease cleaves the TfR mRNA without prior poly(A) tail shortening. However there remains much to learn about this system. The nuclease(s) involved have not been isolated or even partially characterized and the pathway of degradation that follows the endonucleolytic cleavage described here remains totally obscure. An important future goal will be the establishment of an *in vitro* turnover system which would provide an avenue by which some of the unknown aspects of this system can be addressed. Such cell-free systems have begun to yield important information regarding the turnover of several mRNAs (see review by Ross, 1993). With the cleavage site that occurs in intact cells now identified, we are in a position to attempt to characterize further the nuclease responsible for this cleavage.

Materials and methods

RNA isolation

Cells were cultured and treated where indicated with hemin or desferrioxamine as described (Casey *et al.*, 1989). For RNA isolation, cells were washed in phosphate-buffered saline and lysed quickly in ice-cold NP-40 lysis buffer [10 mM Tris−HCl (pH 7.0) 150 mM NaCl, 2 mM $MgCl_2$, 0.5% NP-40]. The supernatant was added to 1.2 vol of SDS solution [10 mM Tris−HCl (pH 7.6) 150 mM NaCl, 5 mM EDTA, 1% SDS] and extracted first with phenol, second with phenol−chloroform−isoamyl alcohol (25:24:1) and third with chloroform. The RNA was ethanol precipitated, washed with 70% ethanol and stored in 10 mM Tris−HCl (pH 7.4) and 5 mM EDTA at −80°C. RNA was fractionated into poly(A)$^+$ and poly(A)$^-$ by oligo(dT) cellulose chromatography as described (Binder *et al.*, 1989). TfR mRNA was analyzed by Northern analysis as described (Sambrook *et al.*, 1989). Northern blots were hybridized with DNA restriction fragments, described in the text, that had been random-primed in the presence of [α-^{32}P]dCTP.

S1 nuclease protection mapping

S1 nuclease protection mapping was performed as described previously (Binder *et al.*, 1989) with modifications. RNA [150 μg of total cytoplasmic RNA or the poly(A)$^+$ or poly(A)$^-$ RNA derived from 150 μg of cytoplasmic RNA] was ethanol precipitated together with 1×10^5 c.p.m. (2×10^6 c.p.m./pmol) of the S1 probe. The S1 probe was made by labeling a synthetic 100mer DNA oligonucleotide at the 3′ end using terminal deoxynucleotidyl transferase (BRL) and [α-^{32}P]ddATP. The DNA oligonucleotide was complementary to nt 3666 to 3756 (all numbering of bases are according to the numbering system for TfR mRNA described in Casey *et al.*, 1988b) and contained 10 additional A residues at its 5′ end. Samples were resuspended in 40 μl of 80% freshly deionized formamide, 0.4 M NaCl, 0.04 M PIPES (pH 6.4) and 0.005 M EDTA, heated at 85°C for 10 min and annealed at 30°C overnight. Samples were diluted with 9 vol of 0.4 M NaCl, 0.03 M sodium acetate (pH 4.8), 0.001 M $ZnCl_2$, 10 μg/ml of sonicated and denatured salmon sperm DNA containing S1 nuclease (1000 units/ml; BRL) and incubated at 37°C for 1 h. Reactions were terminated by addition of EDTA to 0.015 M, were extracted with phenol−chloroform−isoamyl alcohol as described above and ethanol precipitated. Alkaline hydrolysis was performed by resuspending dried samples in 100 μl of 0.2 N NaOH and incubating for 1 h at 42°C. Samples were neutralized with 20 μl of 1 M Tris−HCl (pH 7.4) and 0.2 N HCl and were ethanol precipitated with 10 μg of carrier yeast tRNA. Samples were washed in 70% ethanol prior to electrophoresis in 6% polyacrylamide sequencing gels (Maxam and Gilbert, 1980).

Primer extension

In order to obtain primer extension products that would be short enough to resolve on a 6% sequencing gel, RNA samples were first cleaved at a site ~300 nt 5′ from the primer extension oligonucleotide using oligonucleotide-directed RNase H cleavage. The RNA and cleaving oligonucleotide (nt 2374−2397) were equilibrated in 1×RNase H buffer [200 mM NaCl, 10 mM $MgCl_2$, 1 mM dithiothreitol, 25 mM Tris−HCl (pH 7.5)] for 5 min at 37°C. RNase H (BRL) was added (0.15 to 0.25 units RNase H/μg RNA) and samples incubated for 45 min at 37°C. Reactions were stopped by the addition of SDS to 0.1% followed by one phenol−chloroform−isoamyl alcohol (25:24:1) extraction and ethanol precipitation. RNA pellets were washed with 70% ethanol, dried and resuspended in 7 μl of sterile H_2O. To the RNA, 2 μl of 5×annealing buffer [0.25 M Tris−HCl (pH 8.3) 2.7 M KCl, 0.005 M EDTA] was added and 1 μl of 5′ end-labeled primer (2×10^5 c.p.m., 1.6×10^6 c.p.m./pmol; end-labeled with [γ-^{32}P]ATP and T4 polynucleotide kinase). RNA was denatured by heating at 70°C for 10 min and annealed to the primer by incubating at 50°C for 2 h. For extension reactions, the 10 μl annealing reactions were brought to 40 μl containing final concentrations of 0.7 mM each dATP, dCTP, dGTP and dTTP, 50 mM Tris−HCl (pH 8.3), 5.0 mM $MgCl_2$, 135 mM KCl, 0.25 mM EDTA, 50 ng/μl actinomycin D and 10 units/μl murine MLV-reverse transcriptase (BRL). The extension reactions were incubated at 37°C for 2 h. Reactions were terminated with 260 μl of NET buffer [0.3 M sodium acetate, 10 mM Tris−HCl (pH 7.4), 1 mM EDTA], phenol−chloroform−isoamyl alcohol (25:24:1) extracted and ethanol precipitated. Reactions that contained over 10 μg of RNA were subject to alkaline hydrolysis of RNA, as described above, prior to electrophoresis in 6% polyacrylamide sequencing gels.

Sucrose gradient size fractionation of RNA

RNA was size-fractionated on sucrose gradients as previously described (Uchida *et al.*, 1991). RNA (100 μg) in 100 μl of 10 mM Tris−HCl (pH 7.4), 5 mM EDTA, 0.5% SDS was heated for 10 min at 65°C, briefly chilled on ice and immediately loaded on 10−30% sucrose gradients containing 10 mM Tris−HCl (pH 7.4), 1 mM EDTA and 0.2% SDS. Samples were centrifuged in an SW-41 rotor (Beckman) at 21 000 r.p.m. and 20°C for 19 h. Fractions (1 ml) were collected, diluted with 1 vol of H_2O and ethanol precipitated in the presence of carrier glycogen. RNA pellets were washed in ethanol and stored as described above. Parallel gradients were run in order to assess sucrose concentration by refractive index and to determine the position in the gradient of RNA size markers. RNA from gradient fractions were subjected to primer extension analysis as described above.

Assessment of poly(A) tail length

The poly(A) tails of endogenous TfR mRNA from ARH-77 cells and of TRS-1 and TRS-4 mRNA from the stably transformed mouse B6 fibroblast

cell lines were measured by the method originally described by Brewer and Ross (1988). RNA (5 μg) from ARH-77 cells was hybridized to 25 pmol of the antisense oligonucleotide CL1 (complementary to nt 4583–4597) and cleaved with RNase H (2–4 units, BRL) as described earlier. This reaction cleaves TfR mRNA ~400 nt upstream of the poly(A) tail. Where indicated, the poly(A) tail was removed by including oligo(dT) in the reactions. Samples were electrophoresed through 4% polyacrylamide–urea denaturing gels, electroblotted to nytran and hybridized with a 224 nt antisense [^{32}P]CTP-labeled RNA probe (complementary to nt 4594–4818) that detects the 3′ RNase H cleavage product. RNA transcription and hybridization conditions were as described in the Promega protocol manual. RNA (5 μg) from TRS-1 and TRS-4 cells was hybridized to 50 pmol of the antisense oligonucleotide CL2 (complementary to nt 3750–3759) and treated as described above. The 210 nt 3′ fragment generated by oligonucleotide-directed RNase H cleavage of TRS mRNAs was detected with a ~200 nt [^{32}P]CTP-labeled RNA probe (complementary to the TRS mRNA beginning at nt 3727 and extending into the SV-40 polyadenylation signal contained in the TRS cDNA constructs) as described above.

For measuring the length of the poly(A) tail on both the full-length mRNA and the 3′ endonuclease cleavage fragment, temperature elution from poly(U)–Sephadex was performed. RNA (100 μg) was suspended in 500 μl of 10 mM Tris–HCl (pH 7.4) and 1 mM EDTA, heated to 70°C and then chilled on ice. One volume of 2×binding buffer [0.4 M NaCl, 20 mM Tris–HCl (pH 7.4), 2 mM EDTA and 0.4% SDS] was added and the sample was applied to 0.1 g of poly(U)–Sephadex (GIBCO BRL) that had been prepared as described by the manufacturer. Binding and elutions were performed in batch within a 1.5 ml Eppendorf microcentrifuge tube. Binding occurred by shaking at room temperature for 15 min with the aid of an Eppendorf Thermomixer. The matrix was washed three time by shaking each time with 1 ml of 1×binding buffer for 5 min at 25°C. RNA was eluted at increasing temperature by shaking the matrix with 3 vol of a low formamide-containing elution buffer [50 mM Tris–HCl (pH 7.4), 0.1 M NaCl, 10 mM EDTA, 25% formamide, 0.2% SDS] for 15 min at each successively higher temperature (25, 35, 45 and 55°C). The final elution was performed at 55°C in a high formamide-containing elution buffer [50 mM Tris–HCl (pH 7.4), 10 mM EDTA, 0.2% SDS and 90% formamide] for 15 min with shaking. Samples were diluted with 3 vol of water and were ethanol-precipitated using 50 μg of glycogen as a carrier. Samples were reprecipitated, washed with 70% ethanol and stored in 10 mM Tris–HCl, pH 7.4 and 5 mM EDTA. To measure the length of poly(A) tail on bulk mRNAs eluting in each fraction, 10% of each fraction was 3′ end-labeled using RNA ligase (BRL) and [^{32}P]pCp as described (Krol and Carbon, 1989). Samples were extracted with phenol–chloroform–isoamyl alcohol (25:24:1), ethanol-precipitated, washed with 70% ethanol and resuspended in 10 μl of 10 mM Tris–HCl (pH 7.4) and 10 mM EDTA. RNase A and RNase T1 digestion was performed by adding 200 μl of a 1:100 dilution of solution R (50 U/ml RNase A and 10 000 U/ml RNase T1; Ambion RNase Protection kit) and incubating for 30 min at 37°C. Eluants were ethanol-precipitated with 10 μg of carrier glycogen and washed with 70% ethanol prior to electrophoresis in a 6% polyacrylamide sequencing gel.

Plasmid construction and transfection

Plasmid TRS-41 was constructed by insertion of the *Xba*I–*Bam*HI 250 nt fragment from TRS-4, containing IREs B,C and D that are each missing the 5′ most C of the IRE loop, into the *Xba*I site of TRS-1. This results in a construct containing the TRS-4 and TRS-1 250 nt fragments in tandem, with the TRS-4 cassette 5′ to the TRS-1 cassette. Plasmid TRS-1C$_7$ was constructed by PCR mutagenesis as described (Higuchi *et al.*, 1988). Using this method, the 7 bases corresponding to nt 3727–3733 were mutated from the sequence GAACAAG to CCCCCCC. The PCR product was cloned directly into the *Xba*I–*Bam*HI site of plasmid TRS-1 and confirmed by complete sequencing of the insert. Stable transfectants of TK$^-$ mouse B6 fibroblasts were prepared as described (Casey *et al.*, 1989).

Acknowledgements

We would like to thank Fred Hsieh and Bettina Ackerman for their assistance with certain aspects of this project during participation in the NICHD Summer Student Program.

References

Baker,E.J. (1993) In Belasco,J. and Brawerman,G. (eds), *Control of Messenger RNA Stability*. Academic Press, New York, pp. 367–415.

Baker,E.J., Diener,D.R. and Rosenbaum,J.L. (1989) *J. Mol. Biol.*, **207**, 771–781.

Belasco,J.G. and Brawerman,G. (eds) (1993) *Control of Messenger RNA Stability*. Academic Press.

Bernstein,P. and Ross,J. (1989) *Trends Biochem. Sci.*, **14**, 373–377.

Bernstein,P.L., Herrick,D.J., Prokipcak,R.D. and Ross,J. (1992) *Genes Dev.*, **6**, 642–654.

Binder,R., Hwang.S.-P.L., Ratnasabapathy,R. and Williams,D.L. (1989) *J. Biol. Chem.*, **264**, 16910–16918.

Bohjanen,P.R., Petryniak,B., June,C.H., Thompson,C.B. and Lindsten,T. (1991) *Mol. Cell. Biol.*, **11**, 3288–3295.

Brewer,G. (1991) *Mol. Cell. Biol.*, **11**, 2460–2466.

Brewer,G. and Ross,J. (1988) *Mol. Cell. Biol.*, **8**, 1697–1708.

Brown,B.D. and Harland,R.M. (1990) *Genes Dev.*, **4**, 1925–1935.

Brown,B.D., Zipkin,I.D. and Harland,R.M. (1993) *Genes Dev.*, **7**, 1620–1631.

Buchman,A.R., Burnett,L. and Berg,P. (1980) In Tooze,J. (ed.), *DNA Tumor Viruses*. Cold Spring Harbor Laboratory Press, Cold Spring Harbor, NY, pp. 799–823.

Casey,J.L., Di Jeso,B., Rao,K.K., Klausner,R.D. and Harford,J.B. (1988a) *Proc. Natl Acad. Sci. USA*, **85**, 1787–1791.

Casey,J.L., Hentze,M.W., Koeller,D.M., Caughman,S.W., Rouault,T.A., Klausner,R.D. and Harford,J.B. (1988b) *Science*, **240**, 924–928.

Casey,J.L., Koeller,D.M., Ramin,V., Klausner,R.D. and Harford,J.B. (1989) *EMBO J.*, **8**, 3693–3699.

Greenberg,M.E. and Belasco,J.G. (1993) In Belasco,J. and Brawerman,G. (eds), *Control of Messenger RNA Stability*. Academic Press, New York, pp. 199–218.

Haile,D.J., Hentze,M.W., Rouault,T.A., Harford,J.B. and Klausner,R.D. (1989) *Mol. Cell Biol.*, **9**, 5055–5061.

Harford,J.B. (1993) In Belasco,J. and Brawerman,G. (eds), *Control of Messenger RNA Stability*. Academic Press, New York, pp. 239–266.

Higuchi,R., Krummel,B. and Saiki,R. (1988) *Nucleic Acids Res.*, **16**, 7351–7367.

Horowitz,J.A. and Harford,J.B. (1992) *New Biol.*, **4**, 330–338.

Jaffrey,S.R., Haile,D.A., Klausner,R.D. and Harford,J.B. (1993) *Nucleic Acids Res.*, **21**, 4627–4631.

Klausner,R.D., Rouault,T.A. and Harford,J.B. (1993) *Cell*, **72**, 19–28.

Koeller,D.M., Casey,J.L., Hentze,M.W., Gerhardt,E.M., Chan,L.-N.L., Klausner,R.D. and Harford,J.B. (1989) *Proc. Natl Acad. Sci. USA*, **86**, 3574–3578.

Koeller,D.M., Horowitz,J.A., Casey,J.L., Klausner,R.D. and Harford,J.B. (1991) *Proc. Natl Acad. Sci. USA*, **88**, 7778–7782.

Krol,A. and Carbon,P. (1989) *Methods Enzymol.*, **180**, 212–227.

Laird-Offringa,I.A., De Wit,C.L., Elfferich,P. and Van Der Eb,A.J. (1990) *Mol. Cell. Biol.*, **10**, 6132–6140.

Leibold,E.A. and Guo,B. (1992) *Annu. Rev. Nutr.*, **12**, 345–368.

Liang,H. and Jost,J.-P. (1991) *Nucleic Acids Res.*, **19**, 2289–2294.

Lim,S.-K., Sigmund,C.D., Gross,K.W. and Maquat,L.E. (1992) *Mol. Cell. Biol.*, **12**, 1149–1161.

Littauer,U.Z. and Soreq,H. (1982) *Progr. Nucleic Acid Res. Mol. Biol.*, **27**, 53–83.

Lowell,J., Rudner,D. and Sachs,A.B. (1992) *Genes Dev.*, **6**, 2088–2099.

Malter,J.S. (1989) *Science*, **246**, 664–666.

Maxam,A.M. and Gilbert,W. (1980) *Methods Enzymol.*, **65**, 499–560.

Meinsma,D., Holthuizen,P.E., Van den Brande,J.L. and Sussenbach,J.S. (1991) *Biochem. Biophys. Res. Commun.*, **179**, 1509–1516.

Müllner,E.W. and Kühn,L.C. (1988) *Cell*, **53**, 815–825.

Myer,V.E., Lee,S.I. and Steitz,J.A. (1992) *Proc. Natl Acad. Sci. USA*, **89**, 1296–1300.

Neckers,L.M., Nordan,R., Bauer,S. and Potter,M. (1986) *Curr. Top. Microbiol. Immunol.*, **132**, 148–152.

Roberts,K.P. and Griswold,M.D. (1990) *Mol. Endocrinol.*, **4**, 531–542.

Rosenthal,E.T., Tansey,T.R. and Ruderman,J.R. (1983) *J. Mol. Biol.*, **166**, 309.

Ross,J. (1993) In Belasco,J. and Brawerman,G. (eds), *Control of Messenger RNA Stability*. Academic Press, New York, pp. 417–448.

Ross,J., Peltz,S.W., Kobs,G. and Brewer,G. (1986) *Mol. Cell. Biol.*, **6**, 4362–4371.

Rubin,H.N. and Halim,M.N. (1993) *Int. J. Biochem.*, **25**, 287–295.

Sachs,A.B. (1990) *Curr. Opin. Cell Biol.*, **2**, 1092–1098.

Sachs,A.B. (1993) *Cell*, **74**, 413–421.

Sachs,A.B. and Davis,R.W. (1989) *Cell*, **58**, 857–867.

Sachs,A.B. and Deardorff,J.A. (1992) *Cell*, **70**, 961–973.

Sambrook,J., Fritsch,E.F. and Maniatis,T. (1989) *Molecular Cloning – A Laboratory Manual*. Cold Spring Harbor Laboratory Press, Cold Spring Harbor, NY.

Schuler,G.D. and Cole,M.D. (1988) *Cell*, **55**, 1115–1122.
Shaw,G. and Kamen,R. (1986) *Cell*, **46**, 659–667.
Stern,D.B., Jones,H. and Gruissem,W. (1989) *J. Biol. Chem.*, **264**, 18742–18750.
Stoeckle,M.Y. (1992) *Nucleic Acids Res.*, **20**, 1123–1127.
Stoeckle,M.Y. and Hanafusa,H. (1989) *Mol. Cell. Biol.*, **9**, 4738–4745.
Uchida,S., Kwon,H.M.H., Preston,A.S. and Handler,J.S. (1991) *J. Biol. Chem.*, **266**, 9605–9609.
Vakalopoulou,E., Schaack,J. and Shenk,T. (1991) *Mol. Cell. Biol.*, **11**, 3355–3364.
Vreken,P. and Raué,H.A. (1992) *Mol. Cell. Biol.*, **12**, 2986–2996.
Weber,B., Horiguchi,J., Luebbers,R., Sherman,M. and Kufe,D. (1989) *Mol. Cell. Biol.*, **9**, 769–775.
You,Y., Chen,C.-Y.A. and Shyu,A.-B. (1992) *Mol. Cell. Biol.*, **12**, 2931–2940.

Received on October 7, 1993; revised on January 3, 1994